Infrared Spectroscopy of Solid Hydrogen Sulfide and Deuterium Sulfide

Kristin Fathe, Jennifer S. Holt, Susan P. Oxley, and Christopher J. Pursell*

Department of Chemistry, Trinity University, One Trinity Place, San Antonio, Texas 78212-7200

Received: June 1, 2006; In Final Form: July 31, 2006

The infrared spectra of solid hydrogen sulfide (H_2S) and deuterium sulfide (D_2S) were collected at very low temperatures. Vapor deposition of thin films at the lowest temperature of 10 K produced amorphous solids while deposition at 70 K yielded the crystalline phase III. Infrared interference fringe patterns produced by the films during deposition were used to determine the film thickness. Careful measurement of the integrated absorbance peaks, along with the film thickness, allowed determination of the integrated band intensities. This report represents the first complete presentation of the infrared spectra of the amorphous solids. Observations of peaks near 3.915 and 1.982 μm (ca. 2554 and 5045 cm^{-1}, respectively) may be helpful in the conclusive identification of solid hydrogen sulfide on the surface of Io, a moon of Jupiter.

Introduction

Ice, solid ammonia, and solid hydrogen sulfide are molecular solid cousins with varying degrees of hydrogen bonding.[1] While ice has been studied in great detail, solid ammonia and solid hydrogen sulfide have been less well characterized, especially at very low temperatures (ca. $T < 80$ K).[1−3] Recently, our laboratory began to investigate the physical and chemical properties of these molecular solids using low-temperature infrared spectroscopy.[4] In this report, a study of solid hydrogen sulfide and deuterium sulfide is presented.

While ice and solid ammonia have just one low-temperature (ambient pressure) crystalline phase, hydrogen sulfide has three low-temperature (ambient pressure) thermodynamic crystalline phases.[5,6] These are designated as phases I, II, and III with transition temperatures at 126.2 K (I↔II) and 103.5 K (II↔III) for hydrogen sulfide and at 132.9 K (I↔II) and 107.8 K (II↔III) for deuterium sulfide.[7−9] These thermodynamic phase transitions have been observed as sharp changes in the dielectric constant,[10] heat capacity,[7−9] and NMR line width[7] of the solids. Phases I and II are cubic with four molecules per unit cell and are orientationally disordered. While phase I is face-centered cubic (space group *Fm*3*m* with $a = 5.8486$ Å at 160 K), phase II is primitive cubic (space group *Pa*3 with $a = 5.7647$ Å at 120 K).[6] Upon cooling from phase I to II there is (i) a 2% volume change as the molecules pack more closely together and (ii) a lowering of the orientational disorder. Furthermore, phase I exhibits isotropic motions, while phase II has anisotropic motions.[1] In contrast, phase III is orthorhombic (space group *Pbcm* with $a = 4.0760$ Å, $b = 13.3801$ Å, and $c = 6.7215$ Å at 1.5 K) with eight molecules per unit cell and is orientationally ordered.[6] While earlier reports suggested tetragonal structure, the most recent powder neutron diffraction study[6] indicates an essentially hexagonally close-packed structure with distortions to accommodate the hydrogen atoms. Finally, each phase has a unique proton NMR,[11−13] infrared[14−16] and Raman[17−19] spectra, and X-ray and electron diffraction patterns.[20]

In addition to our interests in comparing the physical and chemical properties of molecular solids, the infrared spectroscopy of low-temperature solid hydrogen sulfide is also of interest because of an ongoing dispute regarding the identification of solid H_2S on Io, a moon of Jupiter. Initially, a peak observed at 3.915 μm (ca. 2554 cm^{-1}) was attributed to the S−H stretching vibration of solid H_2S on the surface of Io.[21] Later, an additional peak at 1.982 μm (ca. 5045 cm^{-1}) was attributed to the first overtone of the S−H stretching vibration.[22] While additional laboratory work[23,24] appeared to support these identifications, other work[25,26] suggested that the peaks were due to solid SO_2, the most abundant molecular species on Io. Further infrared spectroscopic studies of low-temperature hydrogen sulfide therefore seem warranted.

Low-temperature infrared and Raman spectra have been reported for the crystalline phases I, II, and III, with all of the studies involving preparation at $T \geq 65$ K. At lower preparation temperatures, the amorphous solid should be accessible. The amorphous solid is defined as a kinetically trapped, nonthermodynamic, disordered solid or glass. While it is thermally stable for very long periods at low temperatures, upon heating the amorphous solid will convert into the thermodynamically stable crystalline phases. The amorphous phase was not accessible in the previous reports, as the sample crystallizes during formation to one of the crystalline phases, and this order is maintained upon cooling.

This report represents the first detailed study[27] of the low-temperature infrared spectra of solid H_2S and D_2S for the amorphous solid. The infrared spectra of crystalline phase III is also presented for comparison purposes. Integrated band intensities were determined from carefully measured integrated absorbance peaks and film thickness, where the film thickness was determined using an infrared interference technique.

Experimental Section

The experimental system used to study the low-temperature infrared spectra of solid hydrogen sulfide and deuterium sulfide was the same one used earlier for our study[4] of solid ammonia and is similar to a matrix isolation apparatus. Briefly, the system utilized a commercial closed-cycle helium cryostat (Advanced Research Systems, Inc.) with an infrared transparent window (ZnSe) attached to the end of the coldfinger. The temperature of the window was regulated using a silicon-diode sensor and

* To whom correspondence should be addressed. E-mail: cpursell@trinity.edu.

10.1021/jp0634104 CCC: $33.50
Published on Web 08/25/2006

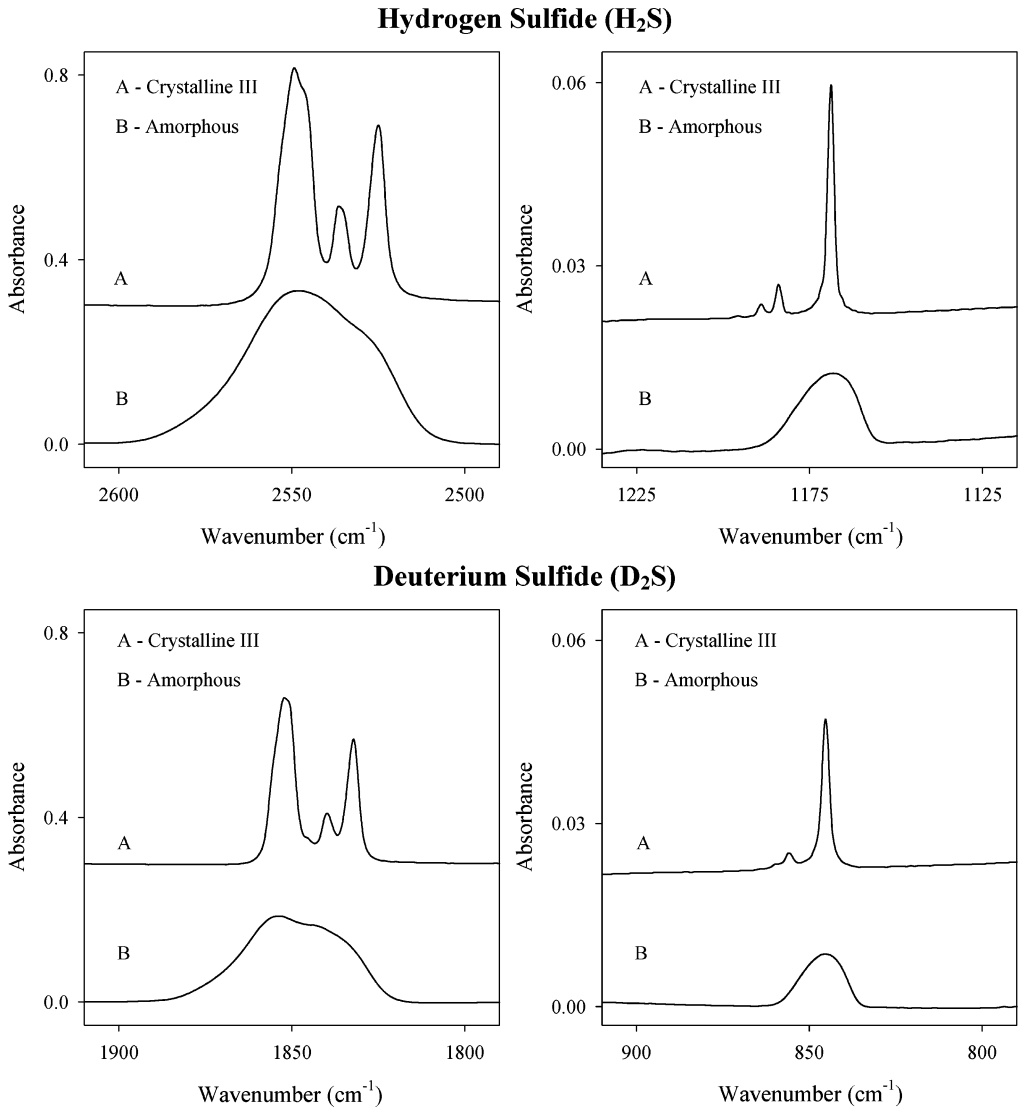

Figure 1. Infrared spectra of solid hydrogen sulfide, H_2S, and deuterium sulfide, D_2S, showing the fundamental stretching and bending peaks. Crystalline phase III films (0.4-μm thick) were vapor-deposited at 70 K, while amorphous films (0.8-μm thick) were deposited at 10 K. The FTIR spectra (100 scans at 2 cm^{-1} resolution) were collected at the deposition temperature and are offset for clarity.

a Lakeshore temperature controller and varied by less than ± 0.1 and ± 1 K for the 70 and 10 K experiments, respectively. In addition to cryopumping, the cryostat was continuously evacuated using a turbomolecular pump attached to the cryostat just above the ZnSe window to minimize condensation of any impurities on the window. The pressure within the cryostat was measured using a cold cathode gauge and was less than 10^{-6} Torr (the gauge was located at the furthest point in the cryostat from the turbomolecular pump and the cold window).

The cryostat was positioned in the sample chamber of a Nicolet Fourier transform infrared (FTIR) spectrometer (Magna 550, range: 500−6000 cm^{-1}) so that transmission spectra of the thin films of solid H_2S and D_2S could be collected. The entire FTIR system, including the region between the walls of the FTIR compartment and the KBr outer windows of the cryostat, was purged with dry, CO_2-free air from a commercial gas generator.

Thin films of solid H_2S and D_2S were prepared by vapor depositing 99.5% pure hydrogen sulfide and 98.0% pure deuterium sulfide (Aldrich Chemical Co.). Gases were introduced directly from a lecture bottle to a glass manifold equipped with a heated capacitance manometer, a liquid nitrogen trap, a diffusion pump, and a mechanical pump. A variable leak valve was used to control the amount of gas sprayed onto the ZnSe window. The rate of deposition was slow and was held constant such that the pressure inside the cryostat remained less than 10^{-6} Torr. The total deposition time was 15−30 min. The deposition temperatures were 10 and 70 K for the amorphous solid films and the crystalline phase III films, respectively. An amorphous film converts to crystalline phase III at 40−50 K. Film thicknesses were determined in situ using an infrared interference technique as the film was deposited.

Results and Discussion

Infrared Spectra. The infrared spectra of thin films of low-temperature solid hydrogen sulfide and deuterium sulfide are shown in Figure 1. Since the molecular symmetry is C_{2v}, one would expect three infrared active bands: one low-frequency bending vibration (ν_2) and two higher frequency stretching vibrations, a symmetric stretch (ν_1) and an asymmetric stretch (ν_3). As displayed in Figure 1, the spectra are in fact dominated by the intense S−H and S−D stretching bands at higher frequency along with the weaker bending band at lower frequency. The peak height of the bending mode is approximately 10−20 times weaker than the stretching modes.

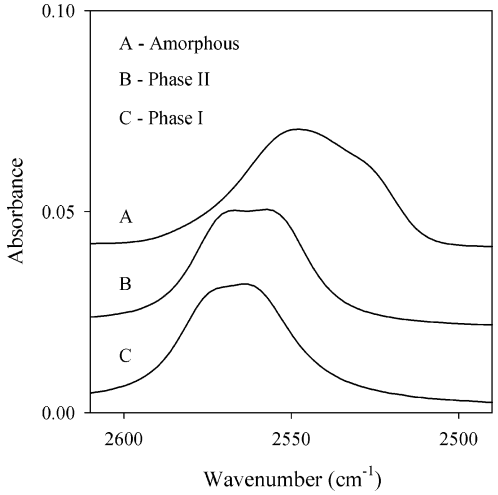

Figure 2. Comparison of the infrared spectra of solid hydrogen sulfide, H_2S, in the S−H stretching region, where the width of the peak is an indication of disorder. (A) Amorphous spectrum was collected at 10 K, (B) crystalline phase II was collected at 110 K, and (C) crystalline phase I was collected at 130 K. The spectra have been normalized (to the same peak height) and offset for clarity.

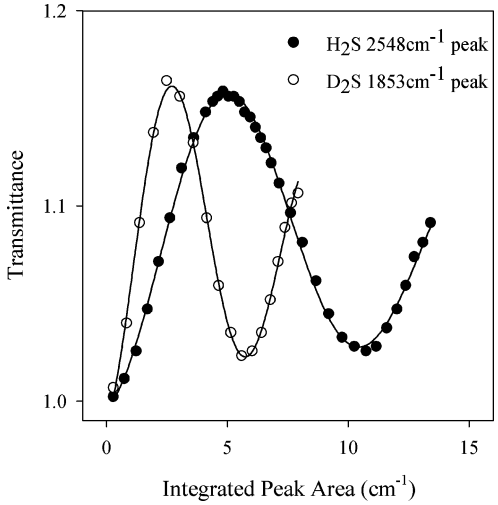

Figure 3. Representative interference fringe pattern for film thickness determination of amorphous H_2S and D_2S at 10 K. The transmittance at 4000 cm^{-1} is plotted against integrated peak area (stretching peak at 2548 cm^{-1} for H_2S and at 1853 cm^{-1} for D_2S) for a vapor-deposited film. Spectra were repetitively collected during the 15−30 min deposition. The lines are a damped sinusoidal fit to the data and give the fringe number, *m*, for the film thickness (see text).

The spectra of the amorphous solids, Figure 1B, are broad and unstructured, consistent with a kinetically trapped, disordered, amorphous molecular solid. The stretching band (ν_1 and ν_3) appears to be made up of at least two peaks, but the band is very broad and unresolved. No attempt was made to deconvolute the band into individual components. For these amorphous solid spectra, the maximum peak positions for the stretching bands are 2548 and 1853 cm^{-1} for H_2S and D_2S, respectively. The isotopic shift is therefore 1.38 and is very close to the expected value of 1.4. The maximum peak positions for the bending bands (ν_2) are 1168 and 846 cm^{-1} for H_2S and D_2S, respectively, giving an isotopic shift of 1.38. All these bands are at approximately the same frequency as the crystalline phase III, but they are considerably broader because of molecular disorder in the amorphous solid. Similar broad bands are observed for the amorphous molecular solid cousins, ice and solid ammonia.[4] Because of these similarities, we assign these spectra to amorphous solid H_2S and D_2S.

Regarding the disorder of the amorphous solid, it is interesting to compare its infrared spectra to the higher temperature crystalline phases, namely, phases I and II, which are known to be orientationally disordered (i.e., S atom ordered, but H atom disordered). As shown in Figure 2, the S−H stretching vibrations for these solids have very similar widths. In particular, their spectral widths (fwhm) are 45, 37, and 35 cm^{-1} for the amorphous and crystalline phases II and I, respectively. Thus, the amorphous solid appears to have slightly greater molecular disorder, as expected.

In contrast to the broad spectral features of the amorphous solids, the crystalline phase III spectra, Figure 1A, are sharp, indicative of ordering in the molecular solid. Furthermore, the symmetric stretching (ν_1) and bending (ν_2) vibrations are split. This splitting is because the solid has eight molecules per unit cell, with two unique sulfur atoms but three unique S−H bonds.[5,6] This nonequivalence leads to splitting of some of the vibrations.[28,29]

For these crystalline phase III spectra, the maximum peak positions for hydrogen sulfide are ν_2 at 1169, 1184, and 1189 cm^{-1}; ν_1 at 2525 and 2536 cm^{-1}; and ν_3 at 2548 cm^{-1}, while for deuterium sulfide they are ν_2 at 846, 856, and 860 cm^{-1}; ν_1 at 1832 and 1840 cm^{-1}; and ν_3 at 1852 cm^{-1}. These values give an average isotopic shift of 1.38. These spectra are in good agreement with previously reported crystalline phase III spectra.[14−16,28]

In addition to these fundamental vibration bands, the low-temperature solid spectra also contain combination and overtone bands, as presented in Tables 1 and 2. Some of these broader and weaker bands have been identified as combination bands involving lattice modes. This identification has allowed a determination of the frequency of these rotational (or librational) and translational lattice vibrations. Using the peak values in Tables 1 and 2, a lattice rotational vibration for the amorphous solid is at 162 and 122 cm^{-1} for H_2S and D_2S, respectively, and a lattice translational vibration is at 94 and 89 cm^{-1} for H_2S and D_2S, respectively. These assignments are based upon comparison to the published[14−16,28] assignments of the crystalline phase III along with the ratio of the frequencies. In particular, the ratio of the libration frequency for the two isotopic species should scale as the square root of the moments of inertia (ca. 1.3−1.4), while the translational frequency should scale as the square root of the molecular masses (ca. 1.06−1.03). For crystalline phase III, using the peak values in Tables 1 and 2, the average lattice rotational vibrations are at 175 and 130 cm^{-1} (frequency ratio = 1.35) for H_2S and D_2S, respectively, while the lattice translational vibrations are at 88 and 86 cm^{-1} (frequency ratio = 1.02) for H_2S and D_2S, respectively. These values for crystalline phase III are in close agreement with previous studies.[14−16,28]

Film Thickness Determination. To determine the integrated band intensities, the film thickness was measured in situ using an infrared interference technique. As the films were slowly vapor-deposited over a 15−30 min period, infrared spectra were repetitively collected. Because of optical interference of the FTIR beam as it passes through the film, the transmittance at a particular wavelength increased and decreased as the thickness of the thin film increased. Also proportional to the film thickness is the integrated peak area of a spectral band, which was measured for each spectrum (using the Nicolet Omnic software) as the film was deposited. The resulting interference fringe pattern is therefore represented by a plot of transmittance versus integrated band area, as shown in Figure 3. For these thickness

TABLE 1: Infrared Spectral Data for Amorphous Hydrogen Sulfide (H_2S) and Deuterium Sulfide (D_2S) at 10 K: Assignments, Peak Positions, and Band Intensities[a]

	hydrogen sulfide (H_2S)		deuterium sulfide (D_2S)	
assignment	position (cm^{-1})	band intensity (10^4 cm^{-1}/mol·cm^{-2})	position (cm^{-1})	band intensity (10^4 cm^{-1}/mol·cm^{-2})
ν_2	**1168**	**6.8**	**846**	**4.9**
$\nu_2 + \nu_R$	1326	3.5	968	1.8
ν_s (ν_1 and ν_3)	**2548**	**501**	**1853**	**256**
$\nu_s + \nu_T$	2642	6.3	1942	4.8
$\nu_s + \nu_R$	2715	0.5		
$\nu_s + \nu_2$	3704	12	2693	4.2
$2\nu_1$	4970	6.6	3629	0.8
$2\nu_3$	5095	13		

[a] The peak position uncertainty is ±2 cm^{-1}, while the average uncertainty in the band intensities is 10% relative standard deviation. The fundamental vibration modes have been bolded. (ν_i notation: 1, 2, 3 = fundamental vibration; s = stretching vibration; R = rotational lattice; T = translational lattice).

TABLE 2: Infrared Spectral Data for Crystalline Phase III Hydrogen Sulfide (H_2S) and Deuterium Sulfide (D_2S) at 70 K: Assignments, Peak Positions, and Band Intensities[a]

	hydrogen sulfide (H_2S)		deuterium sulfide (D_2S)	
assignment	position (cm^{-1})	band intensity (10^4 cm^{-1}/mol·cm^{-2})	position (cm^{-1})	band intensity (10^4 cm^{-1}/mol·cm^{-2})
ν_2	**1169**	**7.0**	**846**	**5.2**
	1184	**0.9**	**856**	**0.5**
	1189	**0.3**	**860**	**0.1**
$\nu_2 + \nu_R$	1347	6.8	982	4.0
ν_1	**2525**	**185**	**1832**	**102**
	2536	**85**	**1840**	**33**
ν_3	**2548**	**405**	**1852**	**203**
$\nu_3 + \nu_T$	2636	12	1938	12
$\nu_3 + \nu_R$	2722	4.3		
$\nu_1 + \nu_2$	3682	2.4	2671	0.9
$\nu_3 + \nu_2$	3694	12	2687	5.3
$\nu_3 + \nu_2 + \nu_R$	3866	2.1	2810	0.6
$2\nu_1$	4955	2.0	3621	1.0
	4968	2.5	3631	1.1
	4982	1.7	3641	0.8
$2\nu_3$	5050	1.7		
	5073	1.6		
	5094	4.3		

[a] The peak position uncertainty is ±1 cm^{-1}, while the average uncertainty in the band intensities is 10% relative standard deviation. The fundamental vibration modes have been bolded. (ν_i notation: 1, 2, 3 = fundamental vibration; R = rotational lattice; T = translational lattice).

measurements, the prominent S−H and S−D stretching bands were used, and the transmittance was measured at both 4000 and 5000 cm^{-1}. The transmittance (T) was then fit to a damped sinusoidal function, such that

$$T \propto \sin(2\pi(\text{area}/b + c)) \quad (1)$$

where b and c are constants of the fit (b is a normalization term of the band area and c is a phase off-set term). The fitting includes a dampening term to account for an overall decrease in transmittance amplitude with film thickness because of increased light scattering from the film. The fringe number m is defined as $m \equiv \text{area}/b$. Once a fringe number was determined for each spectrum (i.e., each data point in Figure 3 corresponds to one spectrum) from the fitting of the transmittance data to eq 1, the film thickness for each spectrum was determined by

$$d = m\lambda/2\eta \quad (2)$$

where d is the film thickness, λ is the wavelength of light, and η is the refractive index of the solid film ($\eta = 1.9$ for T = 63−96 K).[30] As an example, consider the H_2S data in Figure 3, where $m = 1$ appears to occur at an integrated peak area ∼11 cm^{-1}. According to eq 2, (with $\lambda = 2.5 \times 10^{-4}$ cm, $m = 1$, and $\eta = 1.9$), $d = 6.6 \times 10^{-5}$ cm for this peak area. Using this interference method, the film thickness can be measured for each spectrum in the series. On the basis of multiple measurements, the uncertainty in the film thickness is ±10%.

Integrated Band Intensity Determination. To determine the integrated band intensity for each spectral band, the film deposition spectra were used and an integrated peak area for each spectral band (measured with the Nicolet Omnic software) was plotted against film thickness. A representative plot is shown in Figure 4 for the S−H and S−D stretching band of the amorphous solids. This is the same data set used in Figure 3 for determination of the film thickness. Continuing the example above for H_2S, a film thickness of 6.6×10^{-5} cm corresponds to an integrated peak area ∼11 cm^{-1}. The slope (cm^{-1}/cm) of this plot divided by the molar density (0.0343 mol/cm^3)[27] of the solid gives the integrated band intensity (cm^{-1}/mol·cm^{-2}) for that particular spectral band. For the film thickness determination, the S−H and S−D stretching bands were used along with the transmittance at both 4000 and 5000 cm^{-1} (the average thickness was then used for the determination of the integrated band intensities). At least three films of each solid (with a maximum thickness of 1 μm) were examined. The integrated band intensities for each solid are included in Tables 1 and 2.

Identification of Solid H_2S on Io. Solid hydrogen sulfide has been reported to exist in the solid phase on the surface of Io. Weak infrared reflectance bands at 3.915 ± 0.015 μm (ca. 2554 ± 10 cm^{-1})[21] and at 1.9820 ± 0.0005 μm (ca. 5045 ± 1 cm^{-1})[22] were attributed to H_2S frost-deposited on or in sulfur dioxide frost. However, this identification has been questioned and is a source of continued uncertainty.[25,26,31] Some of the

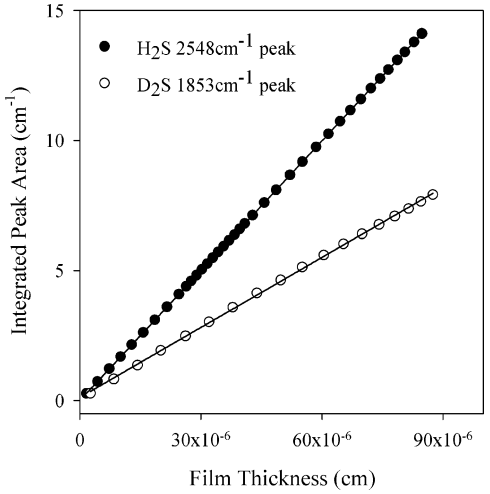

Figure 4. Representative band intensity determination for amorphous H_2S and D_2S at 10 K (same data as in Figure 3). The integrated peak area (stretching peak at 2548 cm^{-1} for H_2S and at 1853 cm^{-1} for D_2S) is plotted against the film thickness, as determined by the fringe pattern data in Figure 3. The lines are a linear fit to the data. The slopes (cm^{-1}/cm) divided by the molar density (mol/cm^3) are the band intensities (cm^{-1}/mol·cm^{-2}) (see text).

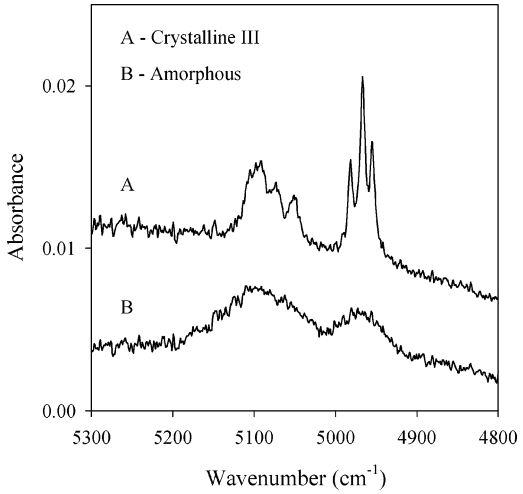

Figure 5. Infrared absorption spectra of hydrogen sulfide, H_2S, in the 1.9820-μm region (ca. 5045 cm^{-1}) for (A) crystalline phase III film at 70 K (1.0-μm thick) and for (B) amorphous film at 10 K (0.9-μm thick). The peaks are due to the first overtone of the S−H stretching vibrations, $2\nu_3$ and $2\nu_1$, respectively. Spectra have been offset for clarity.

uncertainty is due to the uncertainty of the state or phase of the hydrogen sulfide. Is it condensed as pure H_2S or is it condensed on or in the more abundant solid SO_2? Does the H_2S exist as amorphous or crystalline (phase III)?

The S−H stretching vibration of H_2S lies very near to the observed Io peak at 2554 cm^{-1}. Thus, from laboratory studies, Salama et al.[23] reported a strong, broad, absorption peak at 2548 cm^{-1} because of amorphous H_2S at 9 K that appeared to be a good match to the observed Io peak.[27] However, Schmitt and Rodriguez[26] have recently disputed this identification by arguing that solid hydrogen sulfide at 80 K (ca. phase III) has three sharp peaks near 2554 cm^{-1} and is therefore not a good match. As we have presented in detail above, the amorphous spectrum has one broad stretching band at 2548 cm^{-1}, while the crystalline phase III has three sharp peaks at 2525, 2536, and 2548 cm^{-1}. Thus, a reasonable identification for the Io band at 3.915 μm is amorphous H_2S.

Concerning the Io peak at 5045 cm^{-1}, Lester et al.[22] suggested an overtone or combination band of H_2S could account for this peak but did not have experimental support for this suggestion. Additionally, Schmitt et al.[25] did not observe any H_2S transitions above 4000 cm^{-1}, further questioning the source of this peak and the identification of solid H_2S on Io. As clearly shown in Figure 5, the first overtone S−H stretching vibration of solid H_2S, both amorphous and crystalline phase III, does in fact occur near 5045 cm^{-1}. Also, the band intensity is only 40 times less than the fundamental at 2548 cm^{-1} (see Table 1).

Therefore, the 3.915 and 1.920 μm peaks observed in reflectance from Io can be due to H_2S in an amorphous solid state. While the typical temperature on Io (ca. $T = 65-135$ K for nonvolcanic regions)[32] would indicate that the H_2S should be crystalline, Sandford and Allamandola[24] have suggested that H_2S can be trapped in SO_2 surface frost during the cold local night at temperatures below 65 K. If so, the spectral signature due to H_2S might resemble the amorphous solid rather than the crystalline phase III. Future experiments will focus on a detailed infrared analysis of H_2S/SO_2 mixtures at low temperatures.

Conclusion

Infrared characterization of solid H_2S and D_2S has been undertaken at low temperature and pressure. Spectroscopic evidence has revealed the existence of an amorphous solid, similar to that reported for other molecular solids, such as ice and ammonia. Detailed spectral analysis of the amorphous solid and the lowest temperature, thermodynamic crystalline phase III has been presented. This report is the first complete presentation of the infrared spectra of the amorphous solids of H_2S and D_2S. The amorphous spectral peaks are very broad, indicating disorder similar to crystalline phases I and II. Film thicknesses (ca. up to 1 μm) were determined using an infrared interference technique during vapor deposition of the thin films. Measurements of the integrated absorbance peaks then allowed determination of the integrated band intensities.

This report provides definitive evidence for spectral transitions of solid H_2S in the 3.915 and the 1.982 μm regions (ca. 2554 and 5045 cm^{-1}, respectively), consistent with peaks observed from the surface of Io. In particular, for the H_2S amorphous solid, the S−H stretching fundamental occurs at 2548 cm^{-1} and the first S−H stretching overtone occurs at 5095 cm^{-1}. This information should be helpful in the conclusive identification of solid hydrogen sulfide on the surface of Io.

Acknowledgment. The authors would like to gratefully acknowledge the generous funding by the Welch Foundation in support of this research.

References and Notes

(1) Hamilton, W. C.; Ibers, J. A. *Hydrogen Bonding in Solids: Methods of Molecular Structure Determination*; Benjamin Press: New York, 1968.
(2) Hobbs, P. V. *Ice Physics*; Clarendon Press: Oxford, U.K., 1974.
(3) Petrenko, V. F.; Whitworth, R. W. *Physics of Ice*; Oxford University Press: New York, 1999.
(4) Holt, J. S.; Sadoskas, D.; Pursell, C. J. *J. Chem. Phys.* **2004**, *120* (15), 7153.
(5) Fitch, A. N.; Cockcroft, J. K. *J. Chem. Soc., Chem. Commun.* **1990**, *515*.
(6) Cockcroft, J. K.; Fitch, A. N. *Z. Kristallogr*. **1990**, *193*, 1.
(7) Giauque, W. F.; Blue, R. W. *Z. Phys. Chem. Abt B* **1936**, *58*, 831.
(8) Clusius, K.; Frank, A. *Z. Phys. Chem. B* **1936**, *34*, 420.
(9) Kruis, A.; Clusius, K. *Z. Phys. Chem. B* **1937**, *38*, 156.
(10) Symth, C. P.; Hitchcock, C. S. *J. Am. Chem. Soc*. **1934**, *56*, 1084.
(11) Alpert, N. L. *Phys. Rev*. **1949**, *75* (3), 398.
(12) Look, D. C.; Lowe, I. J.; Northby, J. A. *J. Chem. Phys.* **1966**, *44* (9), 3441.
(13) Collins, M. J.; Ratcliffe, C. I.; Ripmeester, J. A. *J. Phys. Chem.* **1989**, *93*, 7495.
(14) Reding, F. P.; Hornig, D. F. *J. Chem. Phys.* **1957**, *27* (5), 1024.

(15) Ferraro, J. R.; Sill, G.; Fink, U. *Appl. Spectrosc*. **1980**, *34* (5), 525.
(16) Ferraro, J. R.; Fink, U. *J. Chem. Phys.* **1977**, *67* (2), 409.
(17) Miller, R. E.; Leroi, G. E. *J. Chem. Phys.* **1968**, *49* (6), 2789.
(18) Anderson, A.; Binbrek, O. S.; Tang, H. C. *J. Raman Spectrosc*. **1977**, *6* (5), 213.
(19) Shimizu, H.; Yamaguchi, H.; Sasaki, S.; Honda, A.; Endo, S.; Kobayashi, M. *Phys. Rev. B* **1995**, *51* (14), 9391.
(20) Harada, J.; Kitamura, N. *J. Phys. Soc. Jpn*. **1964**, *19* (3), 328.
(21) Nash, D. B.; Howell, R. R. *Science* **1989**, *244*, 454.
(22) Lester, D. F.; Trafton, L. M.; Ramseyer, T. F.; Gaffney, N. I. *Icarus* **1992**, *98*, 134.
(23) Salama, F.; Allamandola, L. J.; Witteborn, F. C.; Cruikshank, D. P.; Sandford, S. A.; Bregman, J. D. *Icarus* **1990**, *83*, 66.
(24) Sandford, S. A.; Allamandola, L. J. *Icarus* **1993**, *106*, 478.
(25) Schmitt, B.; de Bergh, C.; Lellouch, E.; Maillard, J.-P.; Barbe, A.; Doute, S. *Icarus* **1994**, *111*, 79.
(26) Schmitt, B.; Rodriguez, S. *J. Geophys. Res.* **2003**, *108* (E9), 5104.
(27) A table of infrared peaks for amorphous H_2S between 1100 and 3800 cm^{-1} was presented in ref 19. However, this table (a) did not include all transitions, (b) did not include band intensities, and (c) contained spectral assignment errors.
(28) Zeng, W. Y.; Anderson, A. *J. Raman Spectrosc*. **2001**, *32*, 9.
(29) Decius, J. C.; Hexter, R. M. *Molecular Vibrations in Crystals;* McGraw-Hill: New York, 1977.
(30) Havariliak, S.; Swenson, R. W.; Cole, R. H. *J. Chem. Phys.* **1955**, *23*, 134.
(31) Nash, D. B.; Betts, B. H. *Icarus* **1995**, *117*, 402.
(32) Matson, D. L.; Nash, D. B. *J. Geophys. Res.* **1983**, *88*, 4771.